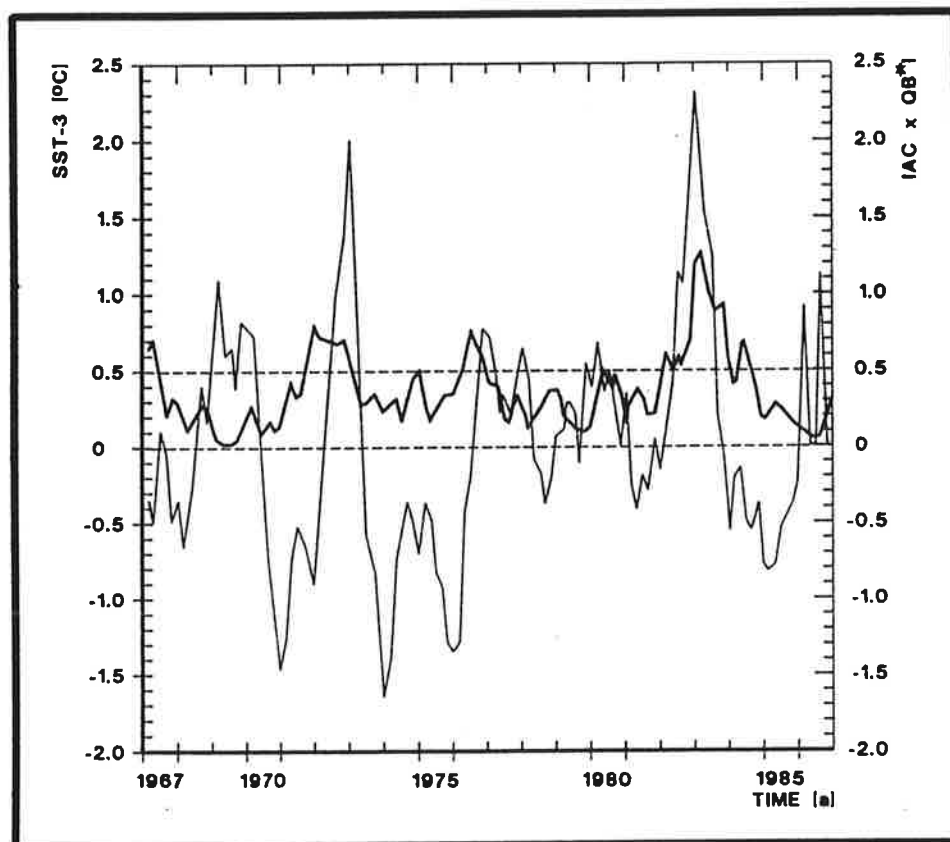




# Max-Planck-Institut für Meteorologie

## REPORT No. 91



### MODAL STRUCTURE OF VARIATIONS IN THE TROPICAL CLIMATE SYSTEM PART I: OBSERVATIONS

by

M. LATIF • T. P. BARNETT • K. MIZUNO

HAMBURG, SEPTEMBER 1992

AUTHORS:

Mojib Latif

Max-Planck-Institut  
für Meteorologie

Timothy P. Barnett

Climate Research Division  
Scripps Institution of Oceanography  
La Jolla  
California 92093  
U.S.A.

Keisuke Mizuno

Far Sea Fisheries Research Laboratory  
Shimizu  
424 Japan

MAX-PLANCK-INSTITUT  
FÜR METEOROLOGIE  
BUNDESSTRASSE 55  
D-2000 HAMBURG 13  
F.R. GERMANY

Tel.: +49 (40) 4 11 73-0  
Telex: 211092 mpime d  
Telemail: MPI.METEOROLOGY  
Telefax: +49 (40) 4 11 73-298

REPb91

MODAL STRUCTURE OF VARIATIONS IN THE TROPICAL CLIMATE SYSTEM  
PART I: OBSERVATIONS

M. Latif  
Max-Planck-Institut für Meteorologie  
Bundesstr.55, D-2000 Hamburg 13, Germany

T. P. Barnett  
Climate Research Division, Scripps Institution of Oceanography  
La Jolla, California 92093, U. S. A.

K. Mizuno  
Far Sea Fisheries Research Laboratory  
Shimizu, 424 Japan

Abstract

We have investigated the modal structure of climate variability in the tropical Pacific by analyzing zonal surface wind stress, sea surface temperature, and upper ocean heat content during the period 1967 to 1986. Three principal climate modes could be identified: The annual cycle, a quasi-biennial (QB) mode, and a low-frequency (LF) mode with a time scale of about 3 years. The annual cycle is mostly governed by the movement of the sun, local air-sea heat exchange and mixing processes. In the eastern equatorial Pacific, the annual cycle involves a westward propagating coupled mode which is caused by processes within the surface mixed layer. The quasi-biennial mode near the equator shows aspects of both mixed layer physics and shallow water wave dynamics and is therefore best described as a "mixed surface/subsurface dynamics" mode. Poleward of 10 degrees local air-sea heat exchange and mixing processes become also important. The low-frequency mode is the traditional ENSO mode, which is best described as the oceanic response to low-frequency atmospheric forcing. Equatorial wave dynamics is crucial for the low-frequency mode.

The quasi-biennial mode shows some evidence for a phase-locking to the annual cycle. However, the period of the quasi-biennial mode is not steady, ranging from about 20 to 30 months during the analysed period. Evidence was found that the annual cycle and the quasi-biennial mode together influence the low-frequency mode such that the low-frequency mode attains maximum amplitude several months after the annual cycle and the quasi-biennial mode were in phase. Our study confirms also the existence of non-linear interactions involving the QB and LF modes of interannual variability only.

## 1. Introduction

Large-scale air-sea interactions play a major role for the generation of climate variability in the tropical Pacific (e. g. Bjerknes (1969)). As described by several authors, these interactions take place on a variety of time scales (e. g. Barnett (1991)). The annual cycle in the eastern equatorial Pacific involves coupled processes (Horel (1982), Philander (1990), Neelin (1991)), as well as the interannual variability. The latter shows variability on a quasi-biennial (QB) time scale (Rasmusson et al. (1990) and at lower frequencies (Rasmusson and Carpenter (1982)). Theoretical and modeling work show that unstable air-sea interactions are possible for a large expanse of model parameter space (e. g. Battisti (1988), Battisti and Hirst (1989), Schopf and Suarez (1988), Philander et al. (1991), Neelin (1991), Neelin and Jin (1992), Neelin et al. (1992)), with quite different spatial and temporal characteristics in different locations of the parameter space. However, although much progress has been made in deriving a theory of air-sea interactions in the tropical climate system, the observational evidence for the validity of certain approximations remains a controversial issue.

Here we investigate the annual and interannual variability in the tropical Pacific to provide a modal description of the observed climate variability. For this purpose we analyzed twenty years of observational data and derived the dominant variability modes. By doing so we cannot only discuss how well these modes are captured by current theory, but also how the different coupled modes interact with each other. Our results indicate that the basic features of the individual coupled modes in the tropical Pacific are well captured by current theory, but our results also suggest that a considerable part of the observed low-frequency variability arises from non-linear interactions between the individual modes. Evidence is found for non-linear interactions between the biennial and low-frequency components of interannual variability (cf Barnett (1991)) and between these two modes and the annual cycle.

This paper is organized as follows. Section two gives a description of the

observational data and the statistical analysis technique. In section 3 we describe the dominant modes of climate variability derived from the data. In section 4 we discuss the interactions between the individual modes. Finally, section 5 gives a summary and discussion of the results.

## 2. Data and analysis technique

### 2.1 Data

It is well known from linear stability analysis that the most important quantities in tropical air-sea interactions are zonal surface wind, sea surface temperature (SST), and upper ocean heat content (e. g. Hirst (1985), Neelin (1991)). We therefore restrict our analysis to these three most important quantities. The analyzed period extends from 1967 to 1986. The SST data are described by Graham and White (1990) and are based on the COADS data set. The zonal surface wind stress was taken from the Florida State University (FSU) data set (Goldenberg and O'Brien (1981), Legler and O'Brien (1984)). As a measure of upper ocean heat content we use the depth of the 20°C-isotherm. This data set is comprised of a re-analysis of the temperature/depth data based upon more than 150.000 vertical profiles of temperature archived at the Japan Far Seas Fisheries Research Laboratory (JFSRL) and at the Scripps Institution of Oceanography (SIO). SST and zonal wind stress cover the domain 124°E to 80°W. The subsurface data were available only for the region 120°E to 140°W. The meridional domain extends from 24°N to 24°S. The data coverage for the 20°C-isotherm data set, especially during the first half of the analyzed period is poor, resulting in large spatial and temporal gaps. We filled these gaps in our analysis by assuming zero anomaly after removing the annual mean value. Since the heat content data were available on a bimonthly basis only, the entire analysis is based on bimonthly data. For this purpose, the monthly SST and zonal stress data were transformed into bimonthly values.

The data were processed in the following way. First, the annual mean was

subtracted from each quantity at each grid point. The data were detrended and each of the quantities was normalized with its spatially averaged standard deviation, so that each quantity has the same weight (and nondimensional units) in the statistical analysis. In order to derive the annual cycle, band-pass filtering was applied retaining variations on time scales of 8 months to 10 years. For the investigation of the interannual variability the annual cycle was removed from the data, and the data were band-passed filtered retaining variability on time scales of 16 months to 10 years. Band-pass filtering was necessary to reduce the problems which arise from the data gaps and from low frequency variability which cannot properly be resolved by our short data set.

## 2.2 Statistical method

Our statistical investigation of the data is based on the method of Principal Oscillation Patterns (POPs) (Hasselmann (1988), Storch et al. (1988), Xu and Storch (1990)), which is designed to extract the dominant modes of variability from a multi-dimensional data set. The POPs are the eigenvectors of the system matrix obtained by fitting the data to a multivariate first order Markov process. POPs are in general complex with real part  $p_1$  and imaginary part  $p_2$ . The corresponding complex coefficient time series satisfies the standard damped harmonic oscillator equation, so that the evolution of the system in the two dimensional POP space can be interpreted as a cyclic sequence of spatial patterns ( $\dots \rightarrow p_1 \rightarrow -p_2 \rightarrow -p_1 \rightarrow p_2 \rightarrow p_1 \rightarrow \dots$ ). The characteristic period to complete a full cycle will be referred to as 'rotation period' and the e-folding time for exponential decay as 'damping time'. Since the two time scales are estimated as part of the POP analysis, narrow band pass filters to identify the different variability modes in the data are not required. We therefore need less 'a priori' information than in other recent studies (Rasmusson et al. (1990), Barnett (1991), Ropelewski et al. (1992)). Further, since we consider simultaneously both atmospheric and oceanic quantities, the POPs can be regarded as the normal modes of the coupled ocean-atmosphere system under the assumption that the coupled system is well represented as a

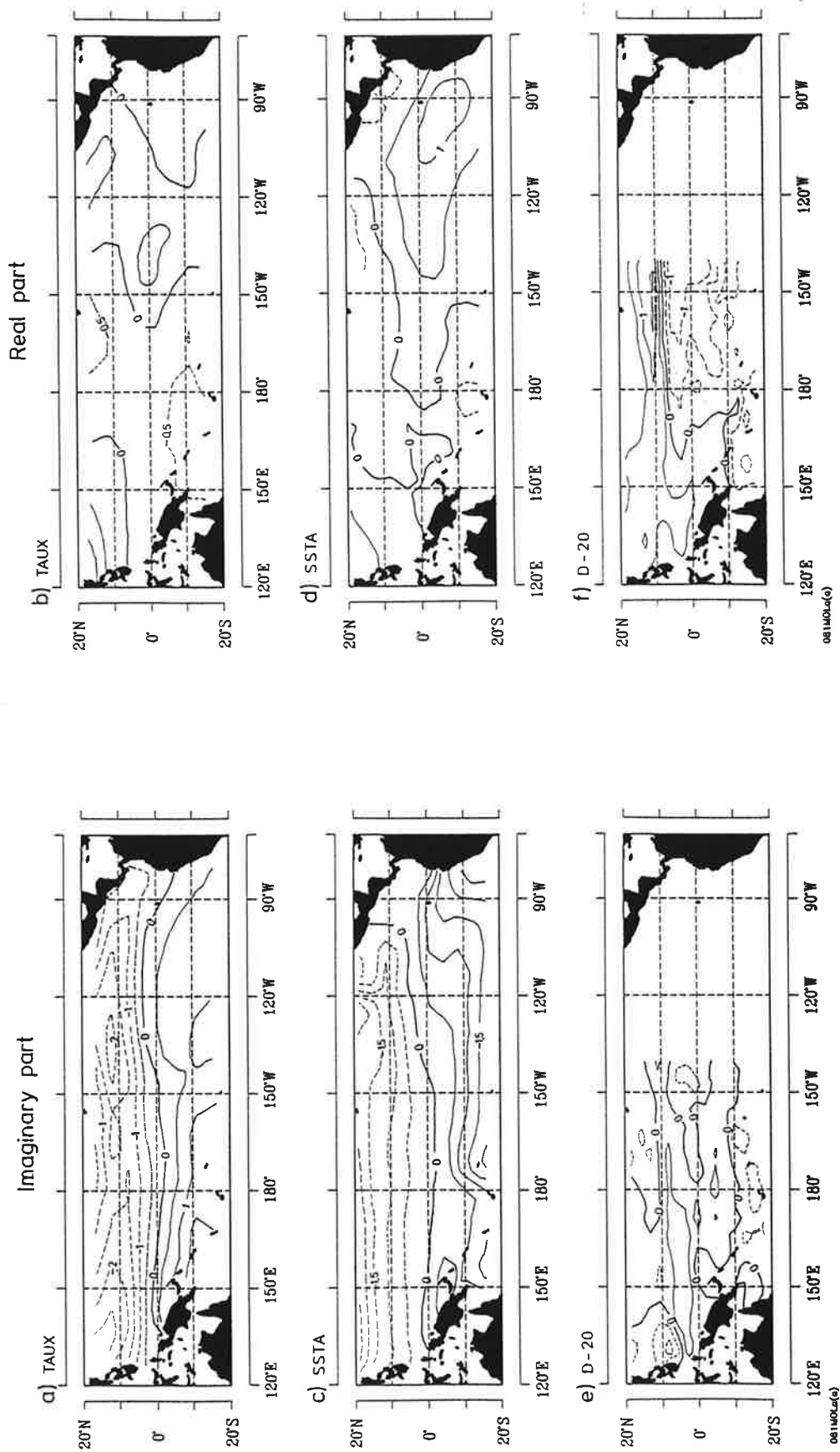


Figure 1: Spatial patterns of the annual cycle POP mode. Left: imaginary part patterns, right: real part patterns.

first order Markow process.

### 3. Normal modes

#### 3.1 Annual cycle

The dominant POP mode of the data describes the annual cycle (Fig. 1). The rotation period of this POP mode is 12 months, the decay time is about six years, and the explained variance amounts to about 51% of the total variance in the band pass filtered data. The POP amplitude time series (Fig. 2a) and the corresponding phase function (Fig. 2b) indicate that the annual cycle evolves fairly regularly. The amplitude of the annual cycle, for instance varies only moderately during the analyzed period, with a maximum/minimum ratio of less than two.

The spatial characteristics of the annual cycle are dominated by a standing component (Fig. 1). The imaginary part of the POP describes the extreme phases of the annual cycle, exhibiting strong north-south asymmetries in zonal surface wind stress (Fig. 1a) and SST (Fig. 1c). The evolution of the annual cycle closely follows the movement of the sun. During northern summer warm surface waters in the Northern Hemisphere go along with weak Trades, while cool SSTs in the Southern Hemisphere go along with strong Trades. This indicates the dominant role of local air-sea heat exchange and mixing processes in determining the SST over the largest portion of the tropical Pacific. No strong signals are found in the 20°C-isotherm data during the extreme seasons. We note, however, the positive signals on both sides of the equator near 5°.

The transition seasons are described by the real part of the annual cycle POP. In general, the real part patterns of zonal wind stress and SST are weak, except in the eastern equatorial Pacific (Figs 1b and 1d). The real part pattern of the depth of the 20°C-isotherm (Fig. 1f) is dominated by a region



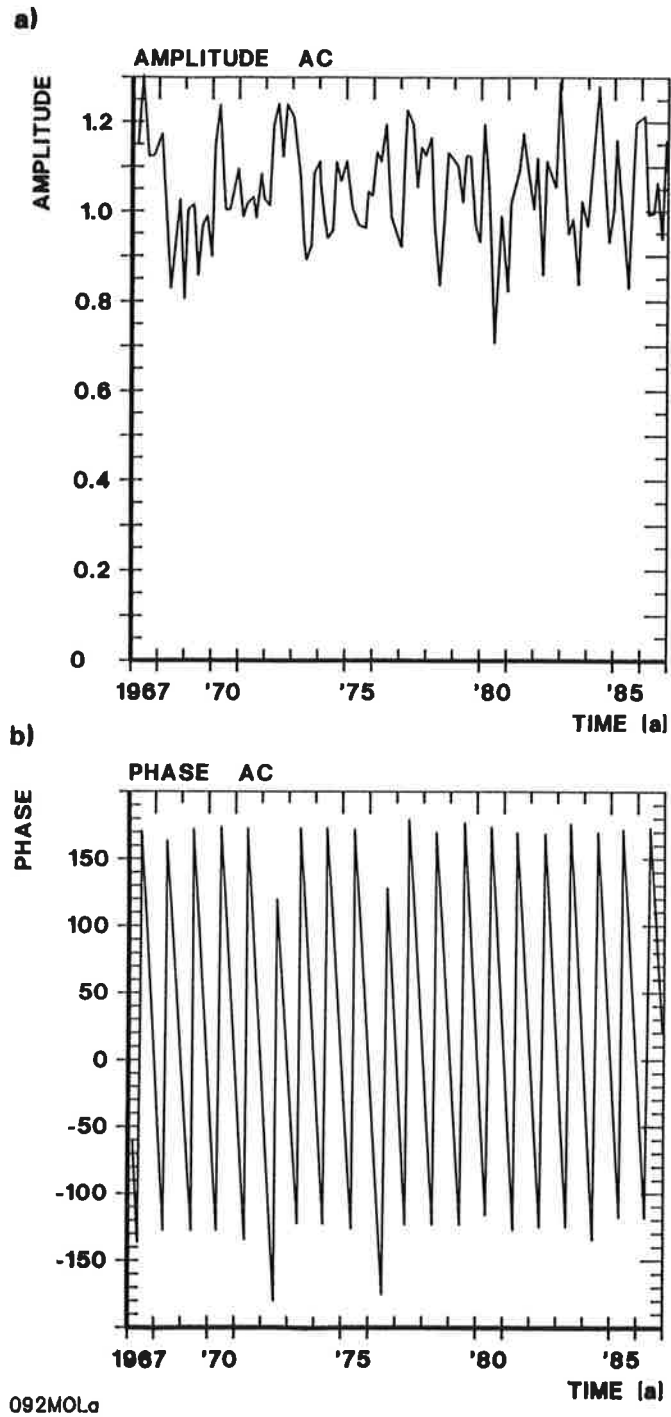


Figure 2: Amplitude (a) and phase (b) time series of the annual cycle POP mode.

of strong meridional gradients in the central Pacific near  $10^{\circ}\text{N}$ . By following the signals in SST and zonal wind stress from the imaginary part (northern summer) to the real part (northern fall) one can identify a westward propagation in these quantities. This westward propagation arises from coupled processes, as described by Philander (1990) and Neelin (1991). The wind stress response appears to be located to the west of the cold water, so that the water is cooled to the west of the coldest water in response to anomalous upwelling and horizontal advection, causing westward propagation. Some evidence of westward propagation is also found in the upper ocean heat content (Figs. 1e and 1f), which is best seen by following the horseshoe pattern near the equator during the rotation from the real part to the (negative) imaginary part pattern. In contrast to White et al. (1990) we did not find any evidence for annual western boundary Rossby wave reflection.

### 3.2 Quasi-biennial mode (QB mode)

In the next step we computed the dominant modes of interannual variability. For this purpose, we removed the annual cycle and band-passed filtered the data, as indicated above. We found two dominant POP modes, one quasi-biennial and one more low-frequency mode, which will be referred to as 'QB' and 'LF' modes, respectively (Barnett (1991)). This is the first time that these two modes have been identified in a multivariate statistical analysis without making use of narrow band-pass filters. We first describe the QB mode which is the second most energetic mode, explaining about 12% of the band-pass filtered data. The rotation period and decay time of the QB mode are both estimated with about 22 months. However, since the time series are not stationary and rather short, estimates of time scales are subject to large uncertainties. As can be seen from the POP phase time series (Fig.4b) the cycle length of the QB mode varies considerably with time, so that the trajectory in the POP phase space (not shown) does not evolve as regularly as theoretically expected. The POP amplitude time series (Fig. 4a) shows strong modulations, exhibiting quiescent as well as active periods. The most active periods occurred during the periods 1972/1973, 1976, and 1982/1983.

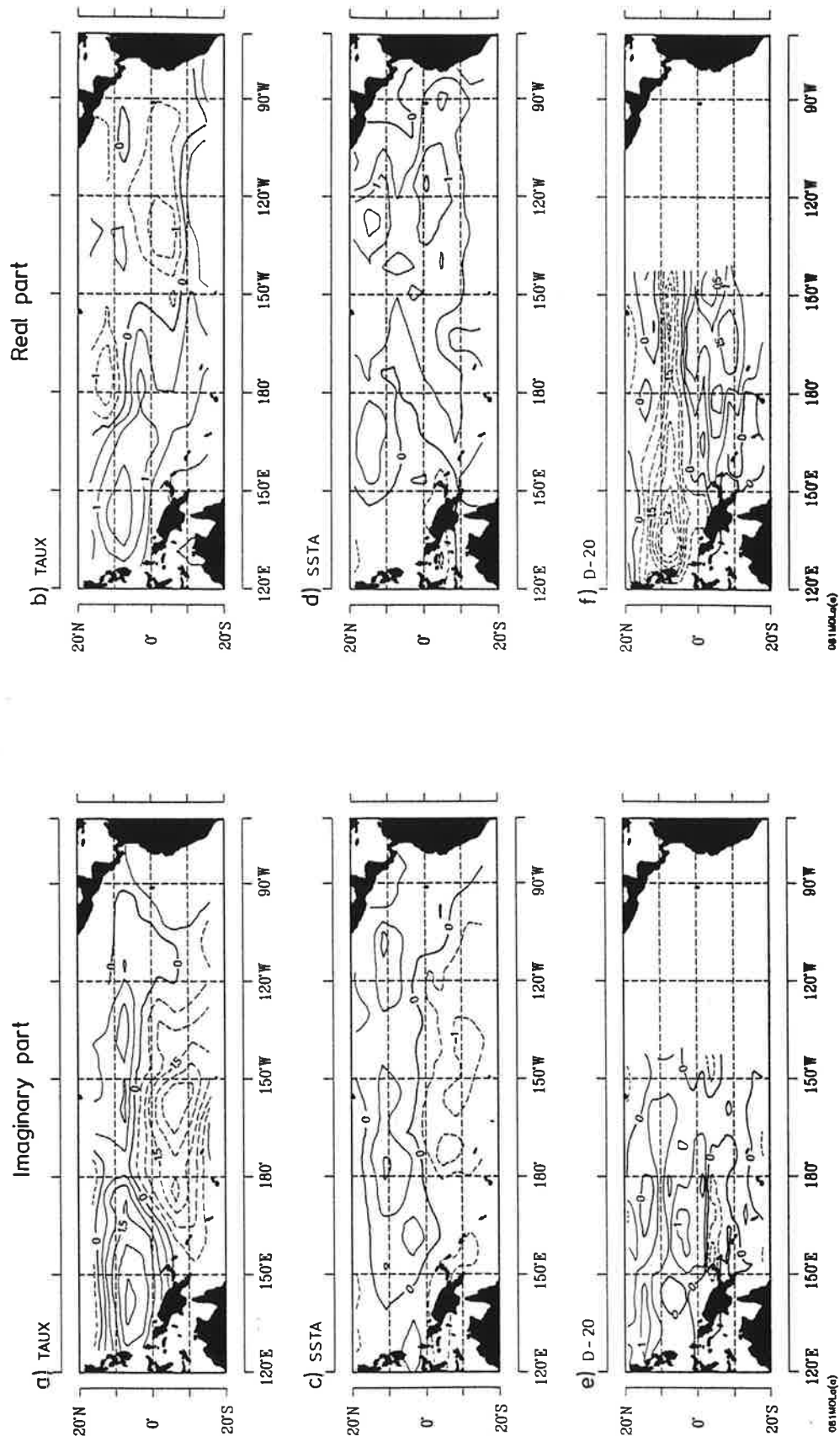
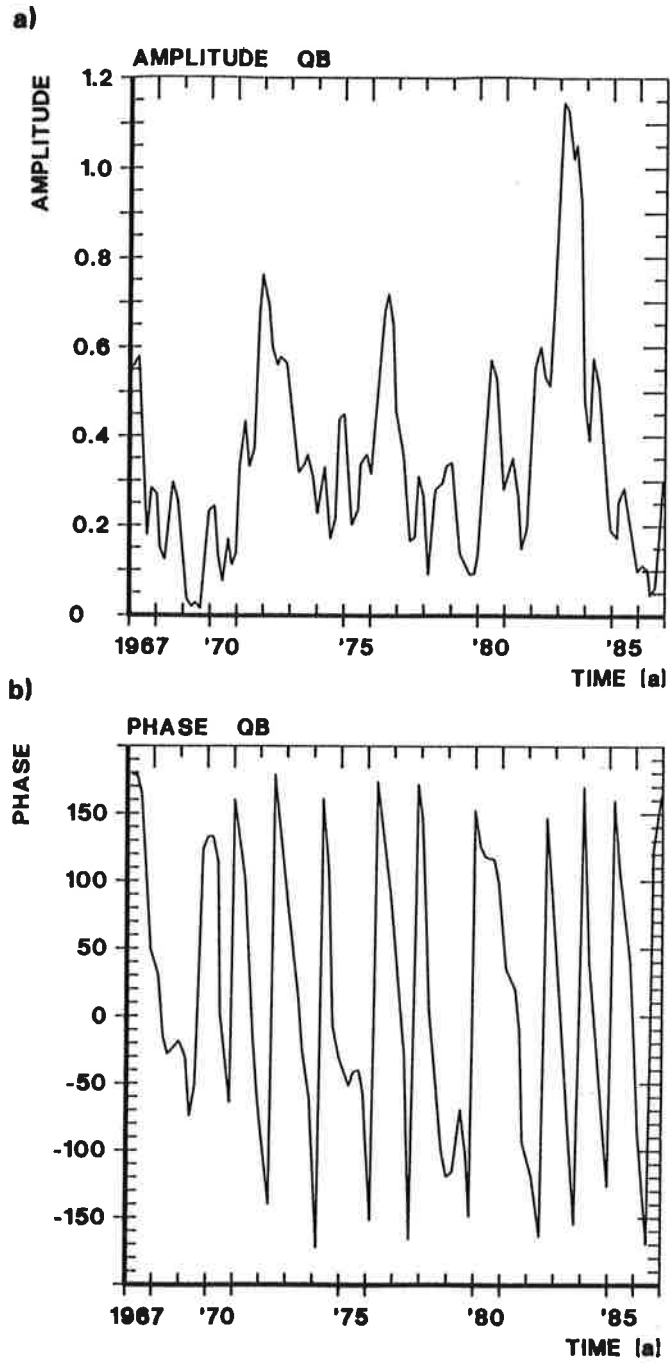


Figure 3: Spatial patterns of the quasi-biennial (QB) POP mode. Left: imaginary part patterns, right: real part patterns.

Near the equator, the spatial characteristics of the QB mode appear to be rather complicated (Fig. 3). The patterns are reminiscent of shallow water dynamics and mixed layer physics. The QB mode is therefore best characterized as a 'mixed surface/subsurface dynamics' mode, using the notation of Neelin and Jin (1992). The real part is characterized by zonal wind stress anomalies which are mostly confined to the near-equatorial region, with westerly anomalies west of and negative anomalies east of  $140^{\circ}\text{W}$  (Fig. 3b). Positive SST anomalies are found in the eastern equatorial Pacific near  $120^{\circ}\text{W}$ , while weak negative SST anomalies are found in the far western equatorial Pacific (Fig. 3d). The upper ocean heat content is dominated by a strong negative anomaly located in the western Pacific near  $10^{\circ}\text{N}$  (Fig. 3f). Further east, positive heat content anomalies are found at and south of the equator. Together, the real part patterns of the QB mode bear some resemblance to an El Niño, i. e. positive SST anomalies in the eastern equatorial Pacific, a Gill (1980) type wind response, and a zonally asymmetric anomalous heat content near the equator. A similar conclusion was drawn by Barnett (1991). The correlation of the corresponding POP coefficient time series with a typical index of anomalous eastern equatorial SST, the SST-3 index (an area average of SST anomalies over the region  $5^{\circ}\text{N} - 5^{\circ}\text{S}$  and  $170^{\circ}\text{W} - 120^{\circ}\text{W}$  which is shown in Fig. 7), however, amounts to only 0.3. Thus the QB described here cannot be regarded as the fundamental ENSO mode, which accounts for most of the ENSO variability. This result is in marked contrast to the study of Ropelewski et al. (1992), who argue that the SST variability in the eastern equatorial Pacific is dominated by its biennial component.

The imaginary part patterns show much more north-south asymmetries in zonal surface stress and SST than the real part patterns. Off the equator, anomalies in these two quantities are out of phase between the two hemispheres and seem to be dominated by local air-sea heat exchange and mixing processes, i. e. strong Trades go along with cool SST and vice versa. In the eastern equatorial Pacific, negative anomalies are found in these two quantities, so that the evolution of the anomalies in this region bears some resemblance to that observed for the annual cycle (Fig. 1), i. e. slow westward propagation along



092MOLb

Figure 4: Amplitude (a) and phase (b) time series of the quasi-biennial (QB) POP mode.

the equator. In the western Pacific, the zonal wind stress anomalies show a pronounced slow eastward propagation, a feature which has been described in many earlier studies (e. g. Barnett (1983), Latif et al. (1990), Rasmusson et al. (1990)). These findings are consistent with the description of the QB mode by Rasmusson et al. (1990). The transition from the real to the (negative) imaginary part yields evidence for western boundary wave reflection and slow eastward propagation at the equator in the anomalous heat content (Fig. 3e).

As shown above, the QB mode shows some aspects of equatorial wave dynamics and of the annual cycle. One may therefore speculate that the QB mode arises from an interaction of the annual cycle with equatorial waves. We shall address this point by analyzing model results in Part II of this paper. Here we investigate, whether the QB mode is locked to the annual cycle. For this purpose, we stratified the zero crossings in the phase time series (Fig. 4b) according to each bimonth. We found that 15 out of the 19 zero crossings occurred during March and August, which provides some (but weak) evidence for phase locking.

### 3.3 Low-frequency mode (LF mode)

The most energetic interannual POP mode, accounting for about 24% of the variance in the band-pass filtered data, has a rotation time of about 40 months and a decay time of about 4 years. This POP mode was already described partly by Latif et al. (1993). The POP coefficient time series of the LF mode indicate a clear relationship to the ENSO cycle (not shown). The zero-lag correlation of the real part POP coefficient time series with the SST-3 index amounts to 0.76, while the lag-8 (months) correlation of the imaginary part is 0.61, with the POP coefficient time series leading the SST-3 index. Thus, the LF mode accounts for most of the ENSO-related variability. This is also supported by the study of Latif et al. (1993), who show that the LF mode can be successfully exploited for ENSO predictions up to lead times of about one year. The amplitude time series of the LF POP (Fig. 6a) exhibits the most energetic times during the periods 1972/1973 and 1982/1983. As for the QB

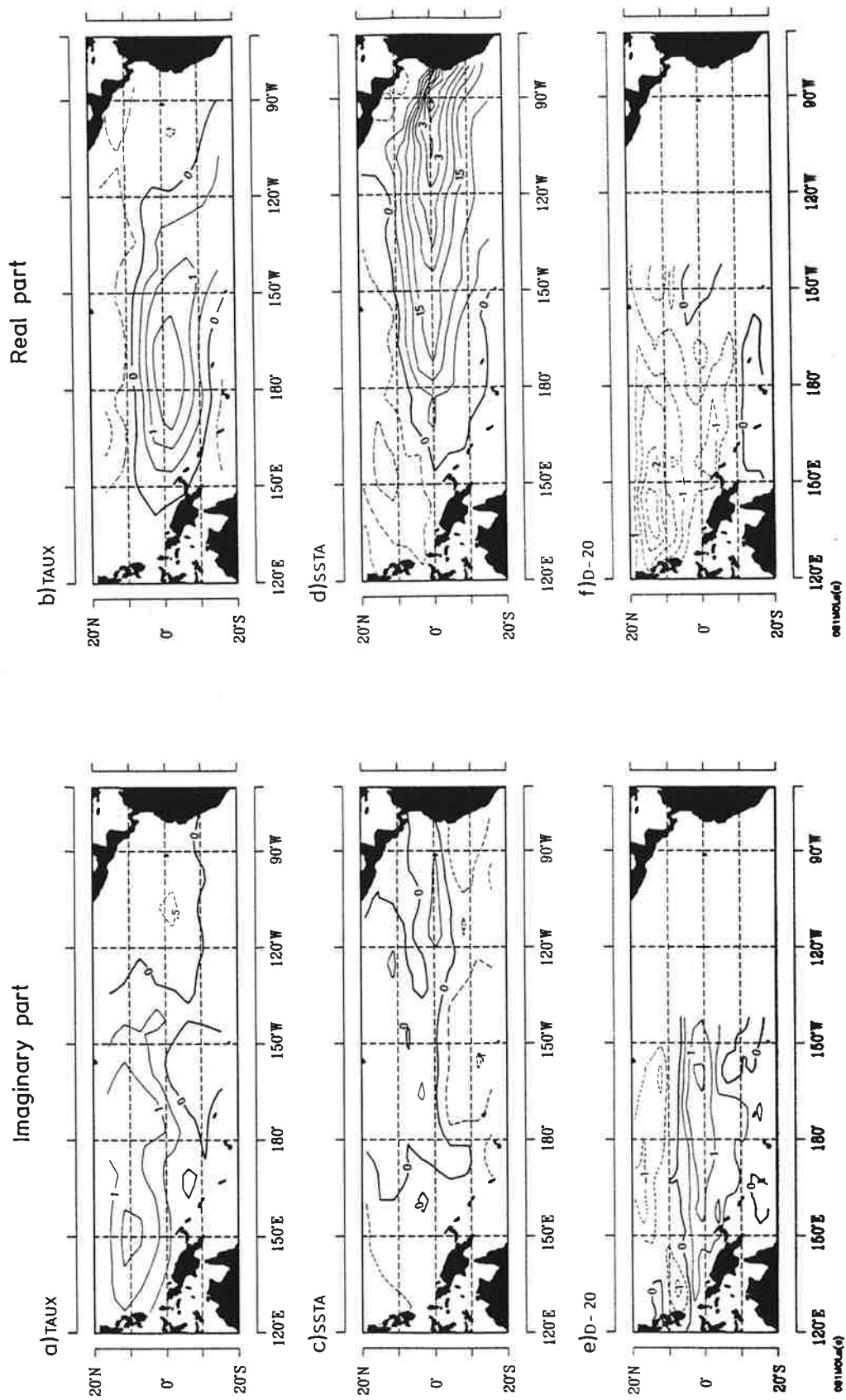


Figure 5: Spatial patterns of the low-frequency (LF) POP mode. Left: imaginary part patterns, right: real part patterns.

mode, the phase time series of the LF mode (Fig. 6b) does not indicate a steady period.

The spatial patterns of the LF mode emphasize its close connection to the ENSO phenomenon (Fig. 5). The real part patterns show the familiar anomaly characteristics observed during the height of the extremes of ENSO (Figs. 5b, 5d, 5f), with maximum SST anomalies in the eastern equatorial Pacific, westerly wind stress anomalies, centered at the equator near the dateline, and the characteristic drop of heat content in the entire western equatorial Pacific. The imaginary part patterns (Figs. 5a, 5c, 5e) show conditions about 10 months earlier. The dominant feature in these 'precursor' patterns is a signal in upper ocean heat content at the equator, centered near 160°W. This signal propagates eastward with a speed of about 25 cm/s, which is about one order of magnitude slower than the gravest baroclinic Kelvin wave speed.

The evolution of anomalies in the LF mode is broadly consistent equatorial wave dynamics as summarized by the conceptual model of 'delayed action oscillation' (Schopf and Suarez (1988), Graham and White (1988), Cane et al. (1990), Chao and Philander (1991)). According to this picture the ocean is not in equilibrium with the atmosphere and has a memory to past winds, as described by Cane and Sarachik (1981). Phase differences between upper ocean heat content on the one hand and SST and wind on the other hand are crucial to maintain the oscillation.

#### 4. Mode interactions

Estimates of time scales, as those by the POP analysis, suffer from the non-stationarity and the short time period of the analyzed time series. An alternative way to estimate the time scales of the different coupled modes makes use of the (amplitude weighted) cumulative phase differences calculated from the corresponding phase time series (Figs. 4b and 6b), which yield time

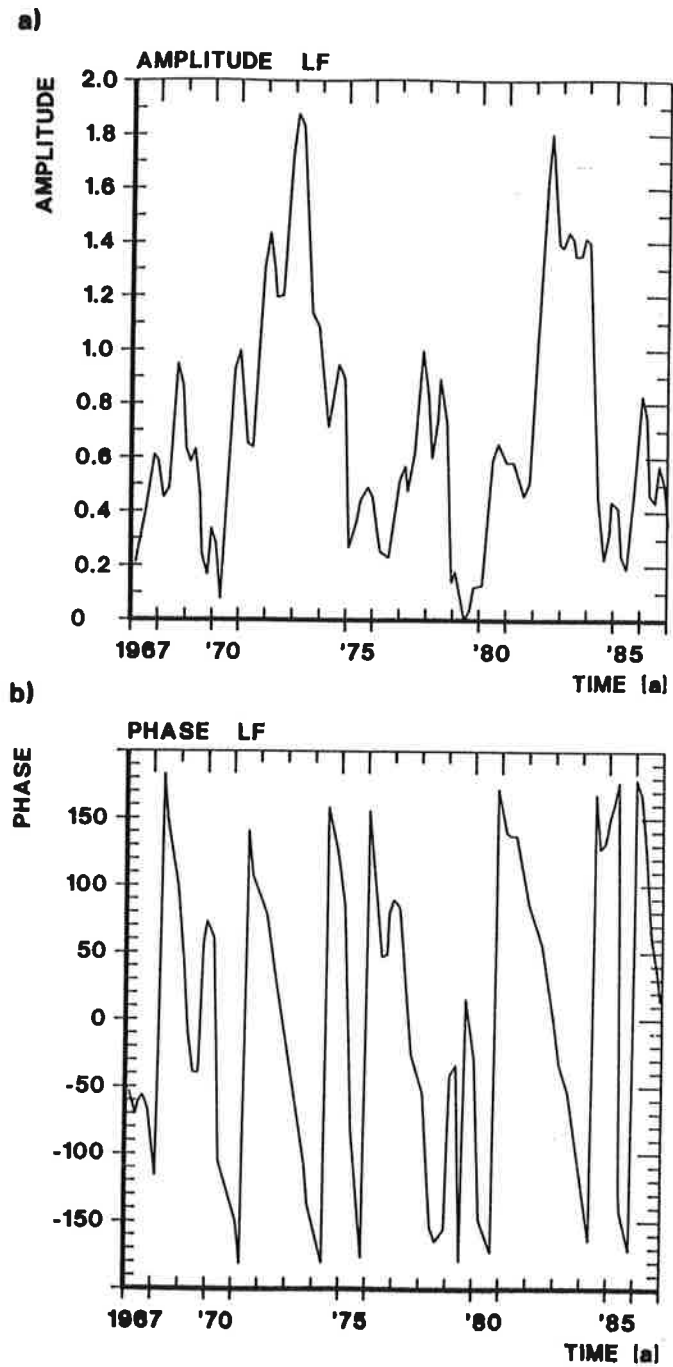


scales of about 21 and 34 months for the QB and the LF mode, respectively. Thus, the time scale for the LF mode is estimated somewhat shorter than the one estimated by the POP analysis. A shorter time scale for the LF mode would give room to the possibility, that non-linear interactions involving all three coupled modes can take place, a possibility which has not been considered before.

Indeed, evidence is found for such an interaction. In Fig. 7a we present the SST-3 time series and the magnitude of the (complex) product of the annual cycle and the QB POPs. Prior to the three warm extremes of the ENSO cycle (1972, 1976 and 1982), the annual cycle and the QB POP mode interfered constructively. It follows from the inspection of the corresponding spatial POP patterns (Figs. 1d and 3d) that the interference at these particular times resulted in an amplification of the annual spring warming and a reduction of the subsequent fall cooling in the eastern equatorial Pacific.

The cold event of 1975, one of the least understood extreme of the ENSO cycle was preceded by an amplified fall cooling in 1974 due to the interference of the QB mode with the annual cycle. However, the interference during this time was less constructive than prior to the three warm extremes. The cold event occurred despite the fact that there was a built-up of warm water in the western equatorial Pacific, as reported by many authors. Prior and during this particular time period the amplitude of the LF mode attained a minimum (Fig. 6a) so that the cold event of 1975 cannot be attributed to variability associated with the LF mode only.

We also computed the (complex) product of the coefficient time series of the QB and LF POP modes and display its magnitude together with the SST-3 index in Fig. 7b. The QB and the LF modes interfered constructively only prior and during the two major warm extremes of 1972 and 1982. Less constructive interference is seen during the mid-seventies prior the 1975 cold event. Was the cold extreme of 1975 caused by non-linear interactions between the different modes? If yes, this example indicates that the changes in equatorial heat content associated with the LF mode can be regarded only as a necessary



092MOLc

Figure 6: Amplitude (a) and phase (b) time series of the low-frequency (LF) POP mode.

but not as a sufficient condition for the occurrence of major anomalies in eastern equatorial SST. Interestingly, ENSO prediction schemes which are based mainly on the low-frequency variations in equatorial heat content, such as those of Cane and Zebiak (1987) and Latif and Graham (1992), failed in hindcasting the 1975 cooling.

In order to further explore the strength of non-linear interactions between the individual coupled modes, we computed non-linear interaction coefficients (complex triple correlations) between the different (complex) POP coefficient time series (a physical interpretation of the non-linear interaction coefficient is given by Barnett (1991)). This objective measure of the strength of non-linear interactions supports our view on the interaction of the different coupled modes. We first computed the interaction coefficient  $[LF, LF, QB^*]$  (the star indicates the complex conjugate of a complex time series), which measures the correlation between the QB mode and the energy of the LF mode. The value of this interaction coefficient amounts to 0.79 which is significant on the 99 % level. The corresponding phase angle of  $-90^{\circ}$  indicates that the LF energy lags the QB mode by several months. This result is in accord with that of Barnett (1991), who used a very different approach to identify the different modes in the tropical climate system.

We then computed the non-linear interaction coefficient  $[LF, QB, AC^*]$  which involves all three coupled modes, including the annual cycle (AC). This non-linear interaction has not been considered in prior studies. The interaction coefficient attains a value of 0.61, which is significant on the 95 % level. Thus, this result supports our hypothesis that prior to major swings in the ENSO cycle, both the annual cycle and the QB mode are important players during the initialization phase of the event. We also computed the value of the interaction  $[QB, QB, AC^*]$ , which measures the phase locking of the QB energy with the annual cycle. The value of this interaction is only 0.30 and therefore supports the conclusion of Barnett (1991) that the QB mode is not simply the first subharmonic of the annual cycle. However, as will be shown in Part II, the seasonal variation in the strength of ocean-atmosphere coupling appears to be fundamental for the origin of the QB mode.

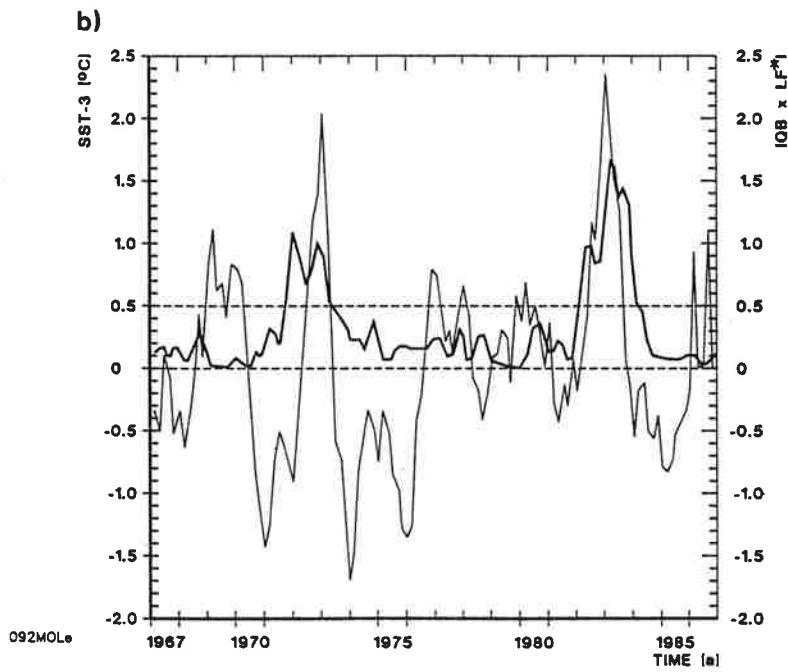
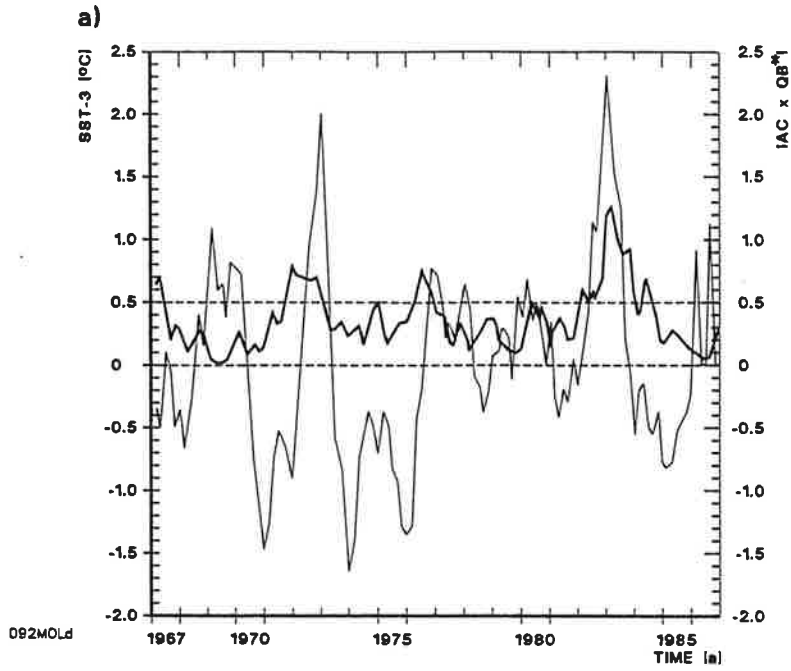


Figure 7: a) SST-3 index of anomalous eastern equatorial SST (thin line) and magnitude of the (complex) product of the annual cycle and the QB POP modes. b) SST-3 index of anomalous eastern equatorial SST (thin line) and magnitude of the (complex) product of the QB and the LF POP modes.

In summary, our results suggest that a significant non-linear interaction exists between the annual cycle and the QB and LF modes of interannual variability. However, this interaction is certainly not the only source of low-frequency variability. There exists an even stronger interaction between the QB and the LF mode. Furthermore, as can be seen from Fig. 7, the tendency of anomalous SST was already positive at the time when interference between the different coupled modes occurred. This suggests that the main role of these non-linear mode interactions is more that of a necessary condition for the occurrence of major events.

## 5. Summary and discussion

We have investigated the coupled modes in the tropical Pacific by analyzing observations from different sources. Three major coupled modes were identified by applying POP analysis, the annual cycle, the quasi-biennial (QB) and the low-frequency (LF) modes of interannual variability. We found evidence for a triple interaction involving all three modes. The constructive interference of these modes appears to be a necessary condition for major extremes in the ENSO cycle. Furthermore, our results supports the existence of a strong non-linear interaction between the QB and the LF modes of interannual variability, as already described by Barnett (1991). A realistic model of interannual variability in the tropical Pacific has therefore to simulate all three coupled modes and to allow for interactions between them.

Current theory captures the basic aspects of the annual and interannual variability near the equator. The annual variability in the eastern equatorial Pacific is governed by processes within the surface mixed layer (Fig. 1), as those described by Neelin (1991). Both SST and zonal wind stress show a distinct westward propagation at the equator, and spatial phase differences between these two variables are crucial for this type of variability. We did not find any evidence for equatorial wave propagation, as previously described

by White et al. (1990). One advantage of the POP analysis is that it separates the different variability modes by time scales. Since the record analyzed by White et al. (1990) was very short and the gravest basin mode of the equatorial Pacific has a time scale close to the annual period, these two modes may not have been separated clearly in their analysis. We conclude here that equatorial wave propagation is unimportant for the annual cycle.

This is completely different for the LF mode of interannual variability, for which equatorial wave propagation is crucial (Fig. 5). The variability in the LF mode can be best described by the conceptual model of 'delayed action oscillation'. According to this picture, processes associated with the subsurface memory of the coupled system are essential and temporal phase differences between upper ocean heat content and both SST and zonal wind stress maintain the oscillation. Ideally, one would expect SST and zonal wind anomalies to behave as standing oscillations, while upper ocean heat content would show slow eastward propagation at the equator. The only feature in the LF mode that is not consistent with this simple view is the slow eastward propagation of zonal wind stress anomalies from the north-western to the central-equatorial Pacific (Fig. 5). By and large, however, the LF mode is also well explained by current theory.

According to stability analysis the variability associated with the annual cycle in the eastern equatorial Pacific and that of the LF mode can be regarded as two extremes, the two modes being well separated in parameter space. While for the annual cycle processes within the surface mixed layer are important and wave processes play a minor role, the opposite holds for the LF mode. As shown by Neelin and Jin (1992), the eigensurfaces of the two modes merge in certain regions of the parameter space, so that "mixed surface/subsurface dynamics" modes can exist over a considerable region of it. We found that the quasi-biennial (QB) mode of interannual variability near the equator is best described by such a mixed mode (Fig. 3), showing aspects of both Ekman and equatorial wave dynamics. The physics behind the QB mode will be further explored in Part II of this paper.

Although our analysis of the interannual variability is consistent with most aspects described in earlier studies (e. g. Rasmusson et al. (1990), Barnett (1991), Ropelewski et al. (1992)), it emphasizes more strongly the contribution of the LF mode to the ENSO-related variability. However, the LF mode described here has a considerably smaller time scale than that assumed in earlier studies and this fact was shown to enable non-linear interactions between all three coupled modes, the annual cycle, the QB and the LF modes of interannual variability. Our analysis, however, suffers from the lack of sufficient data. In particular, the heat content data are very sparse. Furthermore, the length of the used data sets is only 20 years, which is much too short especially in view of identifying non-linear interactions. Therefore this study has to be somewhat speculative in nature. In order to get more insight into the nature of the coupled air-sea modes, we analyzed in addition to the observations model data from different general circulation experiments. Their results are also described in Part II of this paper.

#### **Acknowledgements**

We like to thank Prof. Dr. David Neelin for many fruitful discussions. We are indebted to Dr. Warren White, who provided the 20°C-isotherm data, Dr. Nick Graham, who provided the SST data, and Prof. Dr. J. J. O'Brien and Mr. J. Stricherz, who provided the wind stress data. Many thanks also to Mrs. M. Grunert and Mr. N. Noreiks for drawing the figures. This study was supported by the Körber Project (ML) and by the National Science Foundation through Grant ATM 88-14571-03 (TPB).

## References

- Barnett, T. P., 1983: Interaction of the Monsoon and the Pacific Trade Wind system at interannual time scales. Part I: The equatorial zone. *Mon. Wea. Rev.*, 111, 756-773.
- Barnett, T. P., 1991: The interaction of multiple time scales in the tropical climate system. *J. Climate*, 4, 269-285.
- Battisti, D. S., 1988: The dynamics and thermodynamics of a warming event in a coupled tropical atmosphere/ocean model. *J. Atmos. Sci.*, 45, 2889-2919.
- Battisti, D. S. and A. C. Hirst 1989: Interannual variability in the tropical atmosphere/ocean system: influence of the basic state and ocean geometry. *J. Atmos. Sci.*, 46, 1687-1712.
- Bjerknes, J., 1969: Atmospheric teleconnections from the equatorial Pacific. *Mon. Wea. Rev.*, 97, 163-172.
- Cane, M. A. and E. S. Sarachik, 1981: The response of a linear baroclinic equatorial ocean to period forcing. *J. Mar. Res.*, 39, 651-693.
- Cane, M. A. and S. E. Zebiak, 1987: Prediction of El Niño events using a physical model. In *Atmospheric and Oceanic Variability*. Royal Meteorological Society. James Glaisher House, Grenville Palace, Bracknell, Berkshire, United Kingdom, 182 pp.
- Cane, M. A., M. Münnich, and S. E. Zebiak, 1990: A study of self-excited oscillations of the tropical ocean-atmosphere system. Part I: Linear analysis. *J. Atmos. Sci.*, 47, 1562-1577.
- Chao, Y. and S. G. H. Philander, 1991: on the structure of the Southern



Oscillation and evaluation of coupled ocean-atmosphere models. TOGA Notes, no. 3 (April), 1-8.

Gill, A. E., 1980: Some simple solutions for heat induced tropical circulation. Quart. J. Roy. Met. Soc., 106, 447-462.

Goldenberg, S. O. and J. J. O'Brien, 1981: Time and space variability of tropical Pacific wind stress. Mon. Wea. Rev., 109, 1190-1207.

Graham, N. E. and W. B. White, 1988: The El Niño cycle: A natural oscillator of the Pacific Ocean-Atmosphere system. Science, 240, 1293-1302.

Graham, N. E. and W. B. White, 1990: On the role of the western boundary in the ENSO cycle: Experiments with coupled models. J. Phys. Oceanogr., 20, 1935-1948.

Hasselmann, K., 1988: PIPs and POPs: The reduction of complex dynamical systems using Principal Interaction and Oscillation Patterns. J. Geophys. Res., 93, D9, 11015 - 11021.

Hirst, A. C., 1986: Unstable and damped equatorial modes in simple coupled ocean-atmosphere models. J. Atmos. Sci., 43, 606-630.

Horel, J. D., 1982: On the annual cycle of the tropical Pacific atmosphere and ocean. Mon. Wea. Rev., 110, 1863-1878.

Latif, M., J. Biercamp, H. von Storch, and M. J. McPhaden, 1990: Simulation of ENSO related surface wind anomalies with an atmospheric GCM forced by observed SST. J. Climate, 3, 509-521.

Latif, M., A. Sterl, E. Maier-Reimer, and M. M. Junge, 1993: Structure and predictability of the El Niño/Southern Oscillation phenomenon in a coupled ocean-atmosphere general circulation model. J. Climate, in press.

Legler, D. M. and J. J. O'Brien, 1984: Atlas of tropical Pacific wind stress climatology 1971-1980. Florida State University, Dept. of Meteorology, Tallahassee, U. S. A..

Neelin, J. D., 1991: The slow sea surface temperature mode and the fast-wave limit: analytic theory for tropical interannual oscillations and experiments in a hybrid coupled model. *J. Atmos. Sci.*, 584-606.

Neelin, J. D. and F. F. Jin, 1992: Modes of interannual tropical ocean-atmosphere interactions - a unified view. Part II: Analytical results in the weak coupling limit. *J. Atmos. Sci.*, accepted.

Neelin, J. D., M. Latif, M. A. F. Allaart, M. A. Cane, U. Cubasch, W. L. Gates, P. R. Gent, M. Ghil, C. Gordon, N. C. Lau, C. R. Mechoso, G. A. Meehl, J. M. Oberhuber, S. G. H. Philander, P. S. Schopf, K. R. Sperber, A. Sterl, T. Tokioka, J. Tribbia, S. E. Zebiak, 1992: Tropical air-sea interaction in general circulation models. *Climate Dynamics*, 7, 73-104.

Philander, S. G. H., 1990: A review of simulations of the Southern Oscillation. International TOGA Scientific Conference Proceedings (Honolulu, Hawaii, U. S. A., 16-20 July 1990). World Climate Research Programme, WCRP-43, WMO/TD-No. 379.

Philander, S. G. H., R. C. Pacanowski, N. C. Lau, and M. J. Nath, 1992: A simulation of the Southern Oscillation with a global atmospheric GCM coupled to a high-resolution, tropical Pacific ocean GCM. *J. Climate*, 5, 308-329.

Ramage, C. S., C. W. Adams, A. M. Hori, B. J. Kilonski, and J. C. Sadler, 1980: Meteorological Atlas of the 1972 El Niño, 101 pp. Available from Dept. of Meteorology, University of Hawaii, Honolulu.

Rasmusson, E. M. and T. H. Carpenter, 1982: Variations in tropical sea surface temperature and surface wind fields associated with the Southern Oscillation/El Niño. *Mon. Wea. Rev.*, 110, 354-384.

Rasmusson, E. M., X. Wang, and C. F. Ropelewski, 1990: The biennial component of ENSO variability. *J. Mar. Sys.*, 1, 71-96.

Ropelewski, D. F., M. S. Halpert, and X. Wang, 1992: Observed tropospheric biennial variability and its relationship to the the Southern Oscillation. *J. Climate*, 5, 594-614.

Schopf, P. S. and M. J. Suarez, 1988: Vacillations in a coupled ocean - atmosphere model. *J. Atmos. Sci.*, 45, 549 - 566.

Storch, H. v., T. Bruns, I. Fischer-Bruns and K. Hasselmann, 1988: Principal Oscillation analysis of the 30 to 60 day oscillation in a GCM. *J. Geophys. Res.*, 93, D9, 11022 - 11036.

White, W. B., N. E. Graham, and C.-K. Tai, 1990: Reflection of annual Rossby waves at the maritime western boundary of the tropical Pacific. *J. Geophys. Res.*, 95, C3, 3101-3116.

Xu, J.-S. and H. v. Storch, 1990: Principal oscillation patterns - prediction of the state of ENSO. *J. Climate*, 3, 1316-1329.

Zebiak, S. E. and M. A. Cane, 1987: A model El Niño - Southern Oscillation. *Mon. Wea. Rev.*, 115, 2262 - 2278.

